Volume 12

Washington University Undergraduate Research Digest

Spring 2017

Sonometry for Osteoporosis: Assessing the Impact of Phase Sensitive and Phase Insensitive Detection

Ryan W. Wahidi
Washington University in St. Louis

Sonometry for Osteoporosis: Assessing the Impact of Phase Sensitive and Phase Insensitive Detection

Author:

Ryan W. Wahidi

Ryan is a junior in the College of Arts & Sciences majoring in Physics and Biochemistry. He spent a year working in Dr. James G. Miller's Laboratory for Ultrasonics and plans to pursue a career in medicine.

ABSTRACT

Osteoporosis is a well-characterized disease that leads to structurally deficient bone. Currently, Dual Energy X-ray Absorptiometry (DEXA) is the primary diagnostic tool used to monitor osteoporotic bone tissue. However, quantitative ultrasonic methods should produce more diagnostic information than DEXA, and would reduce patient exposure to radiation. One obstruction to the improvement of bone sonometry is an unexplained sample-thickness dependence of the attenuation coefficient (α). This paper presents physical evidence and simulations of a Lexan™ model system in order to investigate this sample-thickness dependence.

Data was collected by employing a through-transmission substitution technique in a water tank. Experimental results provided phase sensitive data, while simulations for phase sensitive and phase insensitive trials were conducted. Further simulations in which the radius of the receiving aperture was varied were investigated as well. In every scenario, the sample-thickness dependence of α was reproduced. The persistence of the sample-thickness dependence in the simulations suggests that the current methods employed for data acquisition and reduction are not an underlying cause.

KEY TERMS

- Osteoporosis
- Piezoelectric
- Attenuation
- Phase
- Bone Sonometry

FACULTY MENTOR: JAMES G. MILLER, PH.D. ALBERT GORDON HILL PROFESSOR OF PHYSICS

Professor Miller's research focuses on the physics of anisotropic, inherently inhomogeneous media. These systematic studies of the anisotropic properties of the heart have led to fundamentally new insights, has provided the basis for significantly improved diagnostic images of the hearts of patients, and has been incorporated into commercially available echocardiographic imagers in use throughout the world. Miller's publication list includes more than 165 refereed manuscripts, more than 110 conference proceedings and book chapters, and more than 265 abstracts of presentations at national and international meetings. Current investigations include studies of the physics of ultrasound propagation resulting from causality-imposed generalized dispersion relations.

ACKNOWLEDGEMENTS

I would like to thank Dr. James G. Miller for his guidance, support, and inspiration throughout this project. His mentorship and dedication to teaching have been invaluable throughout this work and beyond. We are very grateful to a number of previous members of the Laboratory for Ultrasonics, especially Amber Nelson Groopman and Kirk D. Wallace. The present study made extensive use of experimental data reported by Amber Nelson Groopman and her collaborators and the software package Virtual Tank developed by Kirk Wallace. I would also like to thank the Department of Physics and the Office of Undergraduate Research for financially supporting this research.

Peer Editors:

Syrus Jin, a sophomore majoring in History and Political Science

Madison McManus, a sophomore majoring in Ancient Studies

INTRODUCTION

Fracture resulting from structurally deficient bone often leads to life-altering or life-ending sequelae. The long-term goal of this research is to contribute to the improvement of ultrasonic methods designed to reliably monitor bone composition and strength. Evaluating a course of treatment with pharmacological agents designed to arrest or reverse bone deterioration is one application for such an enhanced bone sonometry system.

Ultrasound is useful in characterizing tissue because wave propagation permits the determination of the physical properties of the tissue of interest. These ultrasonic tissue characterization techniques should offer improved methods for analyzing the physical properties of cancellous bone, permitting the detection of osteopenia and osteoporosis. Osteopenia and osteoporosis are characterized by a decrease in bone mass often associated with high osteoclast activity and low osteoblast activity, causing an individual to become more prone to fractures and other bone-related injuries. The potential for quantitative ultrasound to be used as a diagnostic agent for osteoporosis was demonstrated at least as early as 1984 in a study where the value of attenuation for normal and osteoporotic calcaneus bones were shown to differ (Langton C. et al., 1984). Previous work from our laboratory identified the potential existence of a small but significant "fast wave mode" during ultrasonic propagation through bone, resulting in qualitative and quantitative errors in bone sonometry measurements. Quantitative ultrasonic measurements of potentially osteoporotic bone should in principle yield more diagnostic information than the more widely employed X-ray method, which is known as Dual Energy X-ray Absorptiometry (DEXA). However, current bone sonometry methods at most equal, but do not surpass, the quality of X-ray-based tools.

Although recent methodological improvements introduced by our laboratory seem to offer the potential for significantly enhancing the field of bone sonometry, implementation of these enhanced methods is being impeded by an unexplained sample-thickness dependence for regional values of the attenuation coefficient (α). The goal of our present research is to investigate the scope of this apparent sample-thickness dependence, and develop methods of reducing its impact on bone sonometry.

The phenomenon of phase cancellation at the face of the receiving aperture is a well-known physical effect. One hypothesis is that this phenomenon coupled with the impact of diffraction might be playing a role in the observed apparent sample-thickness dependence of α. The transducers used for sending and receiving signals are piezoelectric devices. The electrical signals sent out by piezoelectric devices are proportional to the instantaneous complex magnitude of the incident ultrasonic field. The pressure field of the ultrasonic wave incident upon a spatially extended piezoelectric receiver can be written:

$$\tilde{P}(x, y, z, \omega) = P_R(x, y, z, \omega) + iP_I(x, y, z, \omega)$$

The magnitude of the piezoelectric response at the frequency ω of a plate located at some point z is:

$$|V_{PE}(z,\omega)| = \left\{\left(\int_{\sigma_R} P_R(x,y,z,\omega)dxdy\right)^2 + \left(\int_{\sigma_R} P_I(x,y,z,\omega)dxdy\right)^2\right\}^{1/2}$$

where σ_R is the face of the receiver. Potential signal loss arising from the integration of the real and imaginary parts of the incident pressure field over the receiver surface can be thought of as an instrumental effect. This effect is instrumental because it depends significantly on the size, placement, and geometry of the receiver. This effect represents signal loss because of the partial cancellation of electrical signals from regions of compressions and rarefactions in the ultrasonic field from different locations on the face of the receiving aperture. Thus, this interference effect is called phase cancellation at the face of the receiving transducer, and is the reason why piezoelectric receivers are phase sensitive.

METHODS

Computer simulations and physical measurements were performed to observe the relationship of the sample-thickness dependence with ultrasonic field diffraction and phase cancellation at the face of the receiving transducer. The computer simulations were carried out through Virtual Tank, a software package created by a former member of our laboratory, Kirk Wallace (Wallace, K. D., 2001).

Data was collected using a through-transmission substitution technique in a water tank. Two 0.5" diameter transducers were aligned on either side of a Lexan™ sample. Lexan™ was chosen for this experiment because it is a tissue-mimicking medium that has well-known ultrasonic indices. Data acquired as part of the present study was supplemented by similar data previously acquired by Amber Nelson Groopman, a former member of our laboratory. One piezoelectric transducer emitted a 2.25MHz signal with a focal length of 55mm, while the other piezoelectric transducer acted as the receiver.

The receiving transducer was attached to the receiver port of a Panametrics 5800 pulser/receiver, whose output was sent to a model 5052B Tektronix digitizing oscilloscope, permitting storage for subsequent off-line analysis. For each measurement, data was acquired from a flat and parallel slab of Lexan™. The Lexan™ slab was initially 30mm in length and was systematically shortened in 2mm steps down to a thickness of 10mm. Signals from a water-only reference path were compared to signals from sample paths for each Lexan™ thickness.

METHODS OF DATA ANALYSIS

To determine the speed of sound of the Lexan™ samples, the Sollish method was employed in which a single transducer is used to both transmit the signal and collect the echoes received. The transducer was aligned perpendicular to the face of a Lexan™ sample with a steel reflector plate placed on the opposite side the sample. Reflections of the signal from the front wall and back wall of the sample, as well as signals reflected by the steel reflector after passing through the Lexan™ sample were collected. By finding the time corresponding to the maximum value of the Hilbert transform for each of these time-domain signals, one can calculate the sample thickness and speed of sound of a sample:

$$d = \frac{c_w}{2(t_{ref} - t_{samp} + t_{BW} - t_{FW})}$$

$$c_{sample} = \frac{c_w\left(1 + t_{ref} - t_{samp}\right)}{t_{BW} - t_{FW}}$$

The apparent attenuation coefficient was determined through a technique known as log-spectral subtraction. Reference path and sample path time domain signals that were captured by the oscilloscope and stored for off-line procession were Fourier transformed to yield their frequency domain equivalents. We model the signal propagation through the sample as a one-dimensional wave

$$A = A_0 e^{-\alpha x} e^{i(\omega t - kx)}$$

where *A* is the amplitude, and *k* is the wave number. The transfer function, H(ω), relates the input signal expressed in the frequency domain to the output signal that has traveled through the sample expressed in the frequency domain. The transfer function can be expressed in terms of the attenuation coefficient, α, phase velocity, c_{phase}, sample thickness, *d*, and the angular frequency, *ω*, which is defined as $2\pi f$, where *f* is the frequency,

$$H(\omega, d) = e^{-a(\omega)d} e^{-id\omega/c_{phase}}$$

With the log spectral subtraction method, the signal loss due to the propagation of the signal through a sample is

$$Signal\ Loss = Power_{ref}(\omega) - Power_{samp}(\omega)$$

The power spectra for the signal path, $Power_{samp}(\omega)$, and the reference path, $Power_{ref}(\omega)$, are proportional to the square of the corresponding frequency domain signals. The signal loss is defined by the difference on a logarithmic scale (that is, the ratio) of the sample and the reference power spectra.

At the front and rear boundaries of the sample, some power is transmitted and some is reflected. The total power loss at the boundaries, T(ω), is determined by expression

$$T(\omega) = 10\log({T^I}_{h\to s} + {T^I}_{s\to h})$$

where ${T^I}_{h\to s}$ and ${T^I}_{s\to h}$ are the intensity transmission coefficients from host medium to sample and sample to host medium, respectively. The intensity transmission coefficients are related to a complex impedance of the material, $\tilde{Z} = \frac{\rho\omega}{k - i\alpha}$. The complex value $\tilde{Z}$ can often be adequately approximated by $\tilde{Z} = \frac{\rho\omega}{k - i\alpha} \approx \rho c_{sample}$ provided that α/κ is sufficiently small.

The relationship between the transmission coefficient and the impedances of the sample and reference media is

$${T^I}_{1\to 2} = \frac{4\left|\tilde{Z}_1 \cdot \tilde{Z}_2\right|}{\left|\tilde{Z}_1 + \tilde{Z}_2\right|^2}$$

where $\tilde{Z}_1$ and $\tilde{Z}_2$ represent the impedances of the sample and host mediums.

The attenuation coefficient in units of dB/unit length can be determined as

$$\alpha(\omega) = \frac{Power_{ref}(\omega) - Power_{samp}(\omega) - T(\omega)}{d}$$

Experimental studies on Lexan™ and a wide range of other plastics indicated that the attenuation rises approximately linearly with frequency in the range of frequencies employed in this study. Consequently, it is common to characterize the attenuation properties by reporting the slope of a least squared fit line to the attenuation coefficient as a function of frequency. That "slope of attenuation" value is often expressed in the form

$$\alpha = \beta f$$

In the field of bone sonometry, the "slope of attenuation" β is termed "normalized Broadband Attenuation" and abbreviated nBUA.

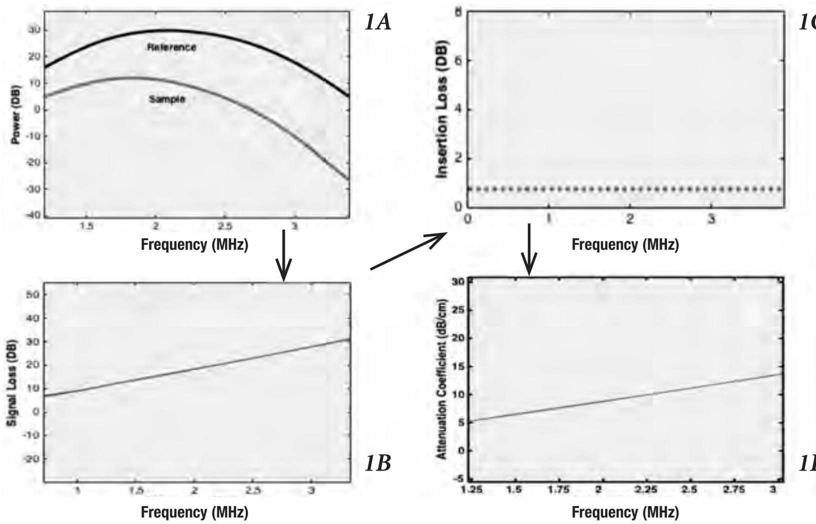

Figures 1A, B, C and D
Summary of obtaining Attenuation coefficient from Reference and Sample Power Spectra.

SIMULATION

Previous work conducted by Dr. Mami Matsukawa's group at Doshisha University in Kyoto, Japan introduced a fruitful approach for evaluating the strengths and limitations of methods to deal with the complexities that result from the presence of overlapping fast and slow ultrasonic waves in cancellous bone (Nagatani et al., 2008). In that work, a sample of cancellous bone was systematically shortened, with through-transmission ultrasonic measurements made at each sample thickness. For the longer lengths, the fast and slow wave modes were sufficiently separated in time such that time-gating could be reliably employed to separate the fast and slow waves, with each mode subsequently analyzed using log spectral subtraction as described above. For intermediate and short thicknesses, conventional time-gating was not feasible. However, a technique introduced earlier by our laboratory making use of Bayesian probability theory had been shown to be capable of separately processing the fast and slow waves in other bone samples. Professor Matsukawa shared the time domain signals captured earlier at her laboratory for those systematically shortened specimens with our laboratory. Amber Nelson Groopman and others from our laboratory applied those Bayesian methods to the Matsukawa lab data.

The results of that analysis were highly encouraging because it was shown that fast and slow waves could be well separated by the Bayesian approach, yielding values for the attenuation properties, phase velocity, and surface losses for each thickness. However, the results showed a small systematic variation of the attenuation properties as a function of sample thickness. After the slow and fast waves were separated using Bayesian analysis techniques, the apparent attenuation coefficient still decreased as a function of sample thickness. Amber Nelson Groopman of our lab demonstrated that this dependence could be replicated using tissue mimicking Lexan™ samples, as shown in *Figure 2* (Groopman, Amber Nelson, 2004).

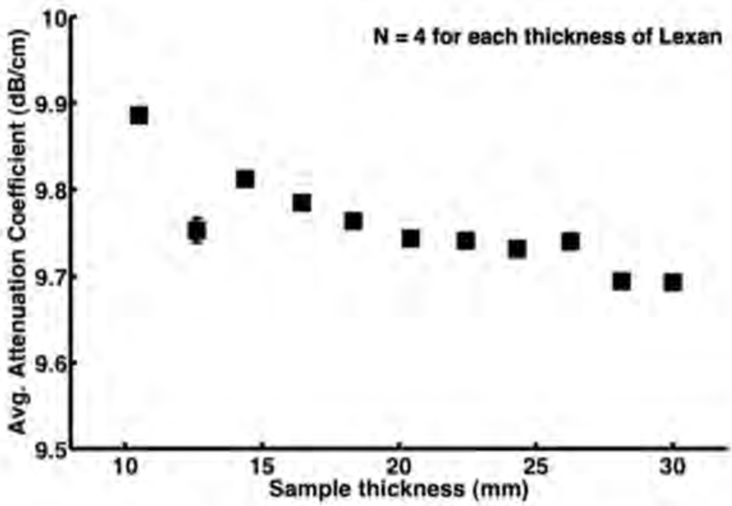

Figure 2
Experimental data demonstrating the unexpected sample thickness dependence of the attenuation coefficient from Amber Groopman.

To determine the scope of this sample thickness dependence on the apparent attenuation, Amber Groopman's experimental work on Lexan™ was simulated using the Virtual Tank software package in the present study. Among other features, Virtual Tank permits visualization of the signal in an azimuthal plane. In *Figure 3*, the three panels on the right show the real part, imaginary part, and magnitude of the signal, respectively.

By placing the transverse plane at twice the focal distance of the transmitting transducer, the right three panels illustrate the amplitude of the signal as it appears on the face of the receiving transducer.

The values for all points on the transverse planes can then be exported as a table of values that represent the amplitude of the signal at each point on the receiving transducer. The local phase of the signal at each point on the receiving aperture is determined by the inverse tangent of the ratio of the imaginary to the real components. For this simulation, the resolution of the receiving transducer was set such that the face could be visualized as a 256x256 table of values.

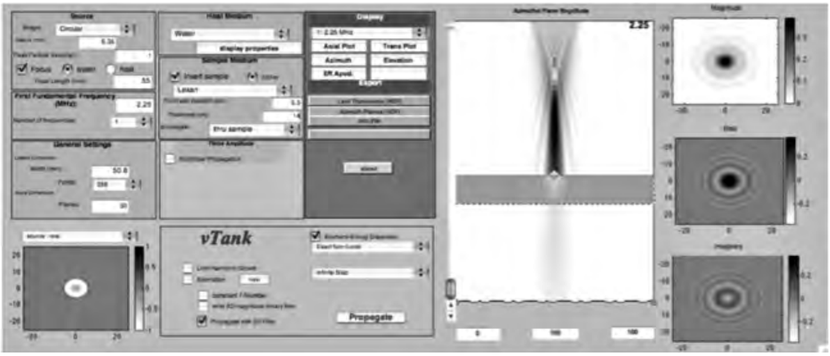

Figure 3
The interface of Virtual Tank

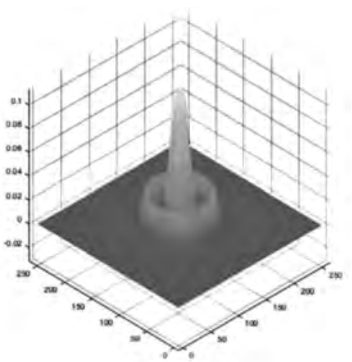

Figure 4A
Real part of the signal at the face of a 1" receiving transducer

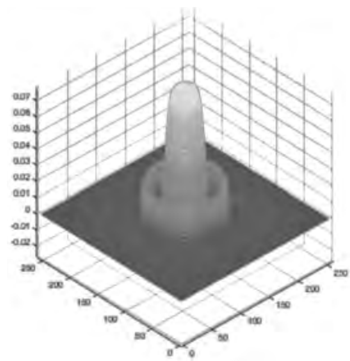

Figure 4B
Imaginary part of the signal at the face of a 1" receiving transducer

The receiving aperture was set to be a square region with 2" on a side. From the stored numerical values, the results that would be obtained with a receiving transducer of any radius up to 2" can be obtained by appropriate masking. From these real and imaginary stored values, the attenuation coefficient can be determined in a phase sensitive manner, yielding results that should be identical to those obtained with the piezoelectric receiving transducers used in the experiment.

The results of the simulation are summarized in *Figures 5* and *6* on the next page. These results correspond to the use of a 12.7mm diameter, 55mm focal length, 2.25MHz center frequency receiving transducer, identical to the transducer used by Groopman.

As shown in *Figure 5*, the agreement between the simulated results and the experimental results is good. The numerical values obtained with simulation are slightly larger (on average approximately 3.5%) than those observed experimentally, perhaps because the value for the slope of attenuation (β) employed in the simulation might be slightly larger than that in the samples studied by Amber Groopman. In *Figure 6*, we show the results

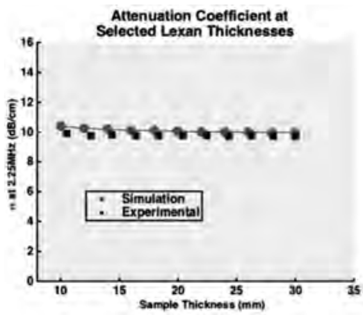

Figure 5

Comparison of experimental data to simulation.

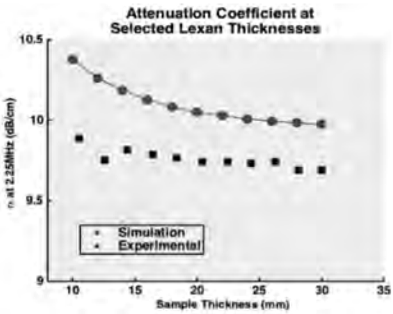

Figure 6

Comparison of experimental data to simulation on an expanded vertical scale.

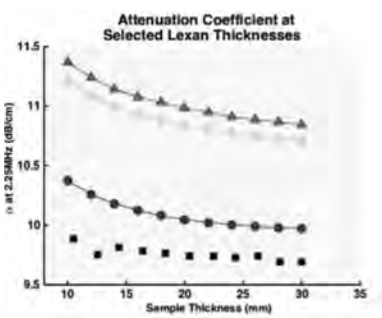

Figure 7

Comparison of attenuation coefficient values obtained from ½" (●), ¼" (◆) and ⅛" (▲) phase sensitive receiving transducers.

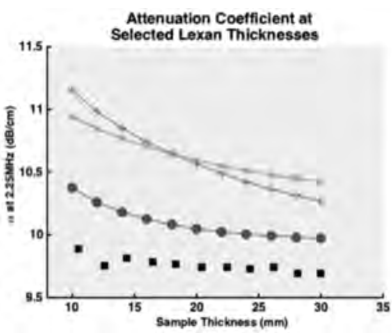

Figure 8

Comparison of attenuation coefficient values obtained from ½" (●), 1" (+) and 2" (×) phase sensitive receiving transducers

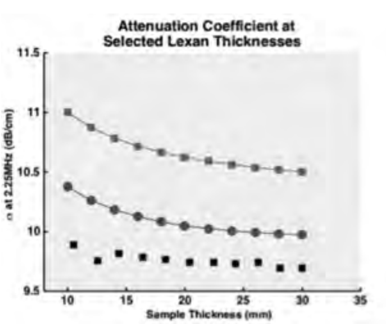

Figure 9

Comparison of experimental data with phase sensitive (●) and phase insensitive (top line ■) simulations

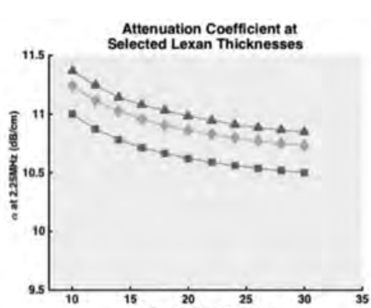

Figure 10

Comparison of attenuation coefficient values obtained from ½" (■), ¼" (◆) and ⅛" (▲) phase insensitive receiving transducers.

with an expanded vertical scale. The data from the simulation follow a trend similar to that observed in the experimental studies by Groopman in that both show an unexpected dependence on sample thickness for a property that should be inherent to the medium and thus independent of the thickness of the sample. In addition, the simulated data differs most from the experimental data at small sample thicknesses. This disagreement may arise in part because the error associated with experimental measurements at small sample thicknesses is significantly larger than that at large sample thicknesses.

Additional simulations were conducted by choosing a range of diameters for the aperture of the receiving transducer. *Figure 7* presents the results for ½", ¼", and ⅛" transducers are presented. The results suggest that smaller receiving apertures can result in errors arising because some of the received signal is missing the receiving aperture, thus producing an overestimate of the attenuation coefficient. Larger diameters of 1"and 2" are considered in *Figure 8*. The resulting overestimate of the attenuation coefficient might be associated with an increase in signal loss resulting from phase cancellation at the face of the receiving aperture. Such losses should increase with increasing aperture, as the simulations in *Figure 8* indicate. In spite of the changes resulting from the use of different receiving apertures, the unexpected trend of slightly decreasing values of the attenuation coefficient as a function of increased sample thickness remains.

In addition to considering phase sensitive piezoelectric receivers, phase insensitive receivers were also considered. This was done in part to determine if removing the effects of phase cancellation at the face of the receiving aperture could eliminate the unexpected sample-thickness dependence of α. Previous work from our laboratory demonstrated that phase insensitive receivers yield more reliable results than phase sensitive (piezoelectric) receivers because the effects of phase cancellation at the face of the receiving aperture are absent. In previous experimental studies conducted in our laboratory, phase insensitive detection was achieved with the use of acoustoelectric transducers made from single crystals of cadmium sulfide (Busse, L. and Miller, J. G., 1981a, 1981b). The results of this phase insensitive analysis are summarized in *Figures 9*, *10*, and *11*.

In *Figure 9*, experimental results obtained with a ½" diameter phase sensitive piezoelectric receiver are compared with simulations for a ½" diameter phase sensitive and ½" diameter phase insensitive receiver. The same unexpectedly small, but systematic decrease with sample thickness is seen for all three results. The fact that the phase insensitive values exceed those obtained with phase insensitive detection will require further investigation.

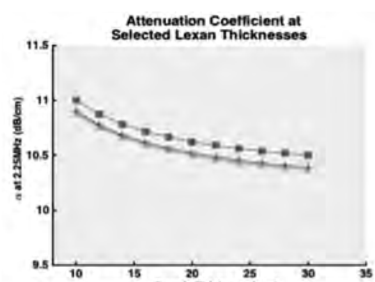

Figure 11
Comparison of attenuation coefficient values obtained from ½" (top line ■), 1" (+) and 2" (×) phase insensitive receiving transducers.

In *Figure 10*, simulations for phase insensitive receivers of ½", ¼", and ⅛" diameter are compared. As anticipated, results for the apparent attenuation coefficient obtained with smaller diameter receivers appear to be larger than those for the ½" receiver, again presumably because a portion of the signal is being missed. In *Figure 11*, results for the apparent attenuation coefficient obtained with larger diameter receivers appear to be slightly smaller than those for the ½" receiver, suggesting that even more of the signal is being captured by the use of large diameter receivers than by the ½" receiver.

The results of the phase sensitive and phase insensitive simulations for a ½" receiving aperture, as well as Groopman's results, are summarized in the following table:

Sample Thickness (mm)	Groopman's Measured Attenuation Coefficient (dB/cm)	Phase Sensitive Simulation Attenuation Coefficient (dB/cm)	Phase Insensitive Simulation Attenuation Coefficient (dB/cm)
10	9.89	10.38	11.00
12	9.75	10.26	10.87
14	9.81	10.18	10.78
16	9.78	10.13	10.72
18	9.76	10.08	10.67
20	9.74	10.05	10.62
22	9.74	10.03	10.59
24	9.73	10.01	10.56
26	9.74	9.99	10.54
28	9.69	9.98	10.52
30	9.69	9.97	10.50

Figure 12
Data table comparing experimental data to simulations obtained with phase sensitive and phase insensitive ½" diameter receiving apertures.

DISCUSSION AND CONCLUSIONS

These studies represent the first successful simulation of the experimental results obtained and reported previously by our laboratory. Good agreement between the simulations and the experimental results was obtained, with agreement to 3.5% for the attenuation coefficient. Furthermore, the unexpected small but systematic variation of the attenuation coefficient with sample thickness that had previously been reported in our experimental data was found in the corresponding simulations. Although only phase sensitive data was available from experimental work, simulations for both phase sensitive and phase insensitive receiving transducers were investigated. Results of simulations for a range of diameters of a phase insensitive receiving transducer were consistent with expectations in that the apparent attenuation coefficient was systematically smaller as a function of increasing diameter. We do not as yet have an explanation for why the apparent attenuation coefficient obtained with phase insensitive detection was not smaller than that obtained with phase sensitive detection.

The observation in simulations of the unexpected systematic dependence of the apparent attenuation coefficient provides strong evidence that that sample-thickness dependence is not an artifact of either the experimental data acquisition system or of the methods of data reduction that had been employed previously. Data reduction in the current investigation employed entirely different methods than those used in the experimental studies. Investigations of the physics underlying the observed sample-thickness dependence are underway.

References

Busse, L. and Miller, J. G. (1981a), "Detection of spatially nonuniform ultrasonic radiation with phase sensitive (piezoelectric) and phase insensitive (acoustoelectric) receivers", J Acoust Soc Am 70(5), 1377–1386.

Busse, L. and Miller, J. G. (1981b), "Response characteristics of a finite aperature, phase insensitive ultrasonic receiver based upon the acoustoelectric effect", J Acoust Soc Am 70(5), 1370–1376.

Groopman, Amber Nelson (2004), "Comparison of Conventional and Bayesian Analysis for the Ultrasonic Characterization of Cancellous Bone", Ph.D. thesis, Washington University in St. Louis.

Langton, C.M., Njeh, C.F. "The measurement of broadband ultrasonic attenuation in cancellous bone—A review of the science and technology". IEEE Trans Ultrason Ferroelectr Freq Control. 2008;55:1546–1554.

Wallace, K. D. (2001), "Characterization of the nonlinear propagation of diffracting, finite amplitude ultrasonic fields", Ph.D. thesis, Washington University in St. Louis.